





Review

A Review of Lithium-Ion Battery Thermal Runaway Modeling and Diagnosis Approaches

Manh-Kien Tran ^{1,*}, Anosh Mevawalla ¹, Attar Aziz ¹, Satyam Panchal ², Yi Xie ³ and Michael Fowler ^{1,*}

¹ Department of Chemical Engineering, University of Waterloo, 200 University Avenue West, Waterloo, ON N2L 3G1, Canada; amevawalla@uwaterloo.ca (A.M.); attar.aziz@uwaterloo.ca (A.A.)

² Department of Mechanical and Mechatronics Engineering, University of Waterloo, 200 University Avenue West, Waterloo, ON N2L 3G1, Canada; satyam.panchal@uwaterloo.ca

³ College of Mechanical and Vehicle Engineering, Chongqing University, Chongqing 400044, China; claudexie@cqu.edu.cn

* Correspondence: kmtran@uwaterloo.ca (M.-K.T.); mfowler@uwaterloo.ca (M.F.)

Abstract: Lithium-ion (Li-ion) batteries have been utilized increasingly in recent years in various applications, such as electric vehicles (EVs), electronics, and large energy storage systems due to their long lifespan, high energy density, and high-power density, among other qualities. However, there can be faults that occur internally or externally that affect battery performance which can potentially lead to serious safety concerns, such as thermal runaway. Thermal runaway is a major challenge in the Li-ion battery field due to its uncontrollable and irreversible nature, which can lead to fires and explosions, threatening the safety of the public. Therefore, thermal runaway prognosis and diagnosis are significant topics of research. To efficiently study and develop thermal runaway prognosis and diagnosis algorithms, thermal runaway modeling is also important. Li-ion battery thermal runaway modeling, prediction, and detection can help in the development of prevention and mitigation approaches to ensure the safety of the battery system. This paper provides a comprehensive review of Li-ion battery thermal runaway modeling. Various prognostic and diagnostic approaches for thermal runaway are also discussed.

Keywords: lithium-ion battery; thermal runaway; battery modeling; fault diagnosis; internal short-circuit



Citation: Tran, M.-K.; Mevawalla, A.; Aziz, A.; Panchal, S.; Xie, Y.; Fowler, M. A Review of Lithium-Ion Battery Thermal Runaway Modeling and Diagnosis Approaches. *Processes* **2022**, *10*, 1192. <https://doi.org/10.3390/pr10061192>

Academic Editor: Antonio Bertei

Received: 30 May 2022

Accepted: 13 June 2022

Published: 15 June 2022

Publisher's Note: MDPI stays neutral with regard to jurisdictional claims in published maps and institutional affiliations.



Copyright: © 2022 by the authors. Licensee MDPI, Basel, Switzerland. This article is an open access article distributed under the terms and conditions of the Creative Commons Attribution (CC BY) license (<https://creativecommons.org/licenses/by/4.0/>).

1. Introduction

The combustion of gasoline or diesel in conventional vehicles is considered one of the leading causes of climate change due to greenhouse gas emissions. Building a future that preserves the environment and reduces dependence on fossil fuels is imperative, and depends substantially on the world's transition to renewable energy. Lithium-ion (Li-ion) batteries are recognized as a sustainable, next-generation vehicle “fuel” owing to their superior features, including high energy density, high power density, long cycle life, low self-discharge rate, no memory effects [1–4], and low environmental emissions and pollution [5,6]. These advantages, especially high energy density and power density, have made Li-ion batteries suitable for successful application in electric vehicles (EVs) [3]. Global EV stock reached 10 million in 2020 and approximately 370 EV models were available worldwide in 2020, representing a 43% and a 40% increase from 2019, respectively [7]. From 2020 to 2025, the global market for Li-ion batteries is estimated to increase from USD 44 billion to USD 94 billion. Moreover, Li-ion batteries are also used in many other energy storage applications, as governments pivot towards the use of renewable energy sources, such as solar and wind, creating a need for energy to be stored.

Despite the remarkable benefits of Li-ion batteries in EVs and energy storage applications, their safety has remained a persistent concern for the public. Li-ion batteries can fail under conditions of abuse, such as overcharge, overdischarge, physical penetration, short-circuit, overheating, accelerated penetration, etc. [8–10]. There are many triggers to

these conditions of abuse, such as fast charging at low and high temperatures, collision and shock, vibration, deformation, metallic lithium plating, formation of lithium dendrite, etc. In addition to these abuse conditions, flammable electrolytes, manufacturing defects, and improper operation can cause failure. Many current Li-ion battery electrolytes are flammable liquids that act as the fuel in battery fires [11]. Although rare, ingress of metallic particulates into the cell during manufacturing can cause an internal short-circuit (ISC) during later usage [12]. Incorrect operation, such as the temperature being too high or low, and overcharging or overdischarging, can lead to accelerated degradation of the active battery materials. The failure of Li-ion batteries typically results in thermal runaway which is a chain reaction of uncontrollable battery temperature and internal pressure increases inside the cell or pack, ultimately leading to gas leakage, fire, and explosion. Much effort has been devoted to thermal runaway modeling to understand its complex mechanisms, as well as to thermal runaway prognosis and diagnosis approaches to prevent and mitigate its catastrophic consequences [13].

The uncontrollable and irreversible nature of thermal runaway is the main challenge for the mitigation of Li-ion battery safety hazards. It has focused researchers' attention on the prediction of thermal runaway behaviors to enable early warning or delays, to potentially prevent thermal runaway in Li-ion battery applications. Thermal runaway modeling is a necessary step in predicting or detecting thermal runaway. The models used are often based on the electrochemical and thermal principles of Li-ion batteries with the goal of simulating temperature and voltage responses during thermal runaway. These models often consider an overall energy balance and involve the development of equations accounting for different sources of heat generation and dissipation.

Since thermal runaway modeling and diagnosis are a crucial part of Li-ion battery advancements, a range of models and diagnosis methods have been studied and developed. Several reviews have focused on the mechanism and diagnosis of ISC of Li-ion batteries [14–16]. Liao et al. [17] conducted a full review of the mechanisms and causes that can lead to thermal runaway, and of approaches to monitoring and detecting thermal runaway in Li-ion batteries. However, there have been many new developments in the field since then, and thermal runaway modeling is a topic that has not been thoroughly reviewed. Researchers have made significant progress in understanding the mechanism and operation of Li-ion batteries, and, consequently, many innovations in battery thermal runaway modeling and diagnosis have emerged. Therefore, there is a crucial need to identify the current and most up-to-date progress of Li-ion battery thermal runaway modeling and diagnosis research. This paper provides a comprehensive review of recent developments in approaches to Li-ion battery thermal runaway modeling, as well as to thermal runaway prediction and detection.

The rest of this paper is organized as follows: Section 2 provides some basic background information on Li-ion battery thermal runaway mechanisms. Section 3 introduces and discusses Li-ion battery thermal runaway models. Section 4 provides a comprehensive review of various thermal runaway prognostic and diagnostic approaches for Li-ion batteries. Finally, some concluding remarks are provided in Section 5.

2. Basic Background on Thermal Runaway Mechanism

A Li-ion battery mainly consists of a cathode, an anode, a separator, and an electrolyte. The cathode is made up of materials that contain lithium compounds and possess a high oxidation-reduction potential, to ensure high battery capacity and output voltage. The anode often has a low oxidation-reduction potential and stable electrochemical properties, to ensure the battery can charge and discharge quickly and have a low self-discharge rate. The separator is a porous film within the battery that prevents active materials of the anode and cathode from reacting directly together in the electrolyte. Its quality can affect the battery capacity, lifespan, and temperature resistance of the battery. The electrolyte, consisting of a salt, an organic solvent, and other additives, is a channel for the migration

of lithium ions between the anode and the cathode. The electrolyte can affect the battery capacity, operating temperature, and power and energy densities.

There are three main types of abuse that lead to thermal runaway, including mechanical, electrical, and thermal [17]. Mechanical abuse involves collision and crush, nail penetrations, compression, etc. Electrical abuse can include overcharging, overdischarging, external short-circuit, etc., while thermal abuse involves overheating, high ambient temperature, fire, etc. These abuse conditions can lead to the collapse of the separator, which can cause an ISC within the battery. The ISC can generate excessive heat and intensify the degree of electrochemical side-reactions, releasing a large amount of flammable gas and leading to increasing internal pressure and expansion of the battery outer case. These effects can ultimately result in a fire or an explosion, causing major safety concerns for users of Li-ion batteries. The flammable liquid electrolytes can be a significant factor in causing fire and explosion. Solid-state electrolytes offer a potential solution to this problem in the future.

The thermal runaway temperature response is usually characterized by three temperatures: T_1 , the onset temperature of detectable battery self-heating; T_2 , the trigger temperature of thermal runaway; and T_3 , the maximum temperature of thermal runaway [18]. The onset of self-heating is due to solid electrolyte interface (SEI) decomposition; T_1 usually occurs when the rate of temperature increase of the battery exceeds an experimentally determined threshold. The trigger for thermal runaway is separator failure leading to an ISC; T_2 is the point where the temperature rises from a constant to a quasi-exponential curve [19]. T_3 can be easily found on a temperature profile as it is the highest point. Some models in published reports simulate a section of the temperature profile, such as from T_2 to T_3 , while other models simulate the complete profile from T_1 to T_3 .

3. Lithium-Ion Battery Thermal Runaway Modeling

3.1. Review of Thermal Runaway Mechanisms and Modeling

Modeling combustion typically involves the coupling of chemistry, transport, and fluid dynamics and is considered extensively in the computational fluid dynamics field. One of the most important considerations is whether the combustion is controlled by chemical kinetics or by turbulent mixing. The non-dimensional Damköhler number is used to determine the flame type. Its form is shown below:

$$Da = \frac{R_a V}{v} = \frac{k/\varepsilon}{\rho_{ad}/R_a} \quad (1)$$

This is the reaction rate over the velocity—it represents the turbulent mixing timescale over the chemical reaction time scale. The turbulent mixing timescale is calculated as the turbulent kinetic energy divided by the rate of dissipation of turbulent kinetic energy. Modeling combustion requires solving the Navier–Stokes equation, a continuity equation, and two additional partial differential equations for k and ε , as well as chemical reaction calculations for enthalpy and mass fractions. However, in the case of batteries, the chemical reaction timescale is smaller (i.e., the chemical reaction rate is large) and consequently the Damköhler number is much greater than 1. This allows for greater simplification of thermal runaway modeling, focusing on chemical kinetics and ignoring computational fluid dynamics with their large computational costs, especially in the turbulent region. Battery thermal runaway models focus instead on the Arrhenius equation for both single and multistep chemical reactions.

Multiple abuse factors lead to thermal runaway, including mechanical stress, internal short-circuit, external short-circuit, elevated temperatures, fast charge, under charge, and overcharge. Internal short-circuits can occur by multiple means from anode/cathode contact to current collector contact and are one of the most dangerous thermal runaway scenarios due to the speed of the reaction. As the battery is still intact, normal catalytic reaction speed is expected, and all the Gibbs free energy of the reaction is converted to heat during Joule heating. The electrolyte subsequently combusts, and further heating occurs.

Undercharge leads to the dissolution of the SEI, leading to gas and stress buildup, while also allowing the electrolyte to react at the electrodes. During overcharge, lithium plating may occur and reduce the electrolyte.

Lithium-ion batteries are sensitive to temperature, and sub-optimal temperatures can lead to degradation and thermal runaway. At temperatures above 80 °C, the SEI layer begins to break down [20]. With the protective SEI layer broken, the lithiated carbon can now react and reduce the electrolyte; this is an exothermic reaction that occurs at temperatures around 100 °C with the reaction peaking at 200 °C [20,21]. At temperatures above 110 °C, the electrolyte begins to break down, and, at temperatures above 135 °C, the separator melts [22]. The electrolyte evaporates at 140 °C and the vapors of the organic electrolyte combust readily in the presence of oxygen [21]. Since oxygen is released from the decomposition of the cathode at high temperatures (200–230 °C), it is a high-risk scenario, and the temperature of the Li-ion batteries must be controlled [20]. Thermal runaway is a major concern for lithium-ion batteries. Elevated temperatures in batteries can trigger exothermic reactions which lead to a further increase in temperature and more deleterious reactions. Previous studies have shown that the onset of thermal runaway varies with the state of charge (SOC) and the voltage. For LiCo₂ batteries, the onset of thermal runaway occurs at 144 °C for 2.8 V, at 109 °C for 3.0 V, and at 104 °C for 4.06 V [21].

Huang et al. [23] discuss various safety measures, including relief valves, novel separators, flame retardant additives, current interrupt devices (CID), and positive thermal coefficient (PTC) devices. They state that Li-ion battery failure is always triggered by successive exothermic side-reactions, such as SEI layer decomposition, separator melting, cathode/anode reactions with the electrolyte, and electrolyte decomposition. Liu et al. [24] measured the total energy of combustion of a 18,650 battery and found that it was almost three times that of the electrical energy alone. Some studies have found that large format cells have a higher risk of jet fires and explosions, especially at high states of charge, as large cells possess more energy and have larger temperature gradients between the cell surface and the interior [25,26].

Figure 1 shows four distinct regions. A sudden voltage drop is seen once the separator has melted and the two electrodes make contact. As the electrodes are solid and the electrolyte moisture concentration is low, the reaction is not immediate as solid-state reactions are typically slow. At elevated temperatures, however, solid-state reactions with low moisture content can produce material stuck in the transition state representing a dangerous phenomenon. The four regions in Figure 1 are explained further in Figure 2.

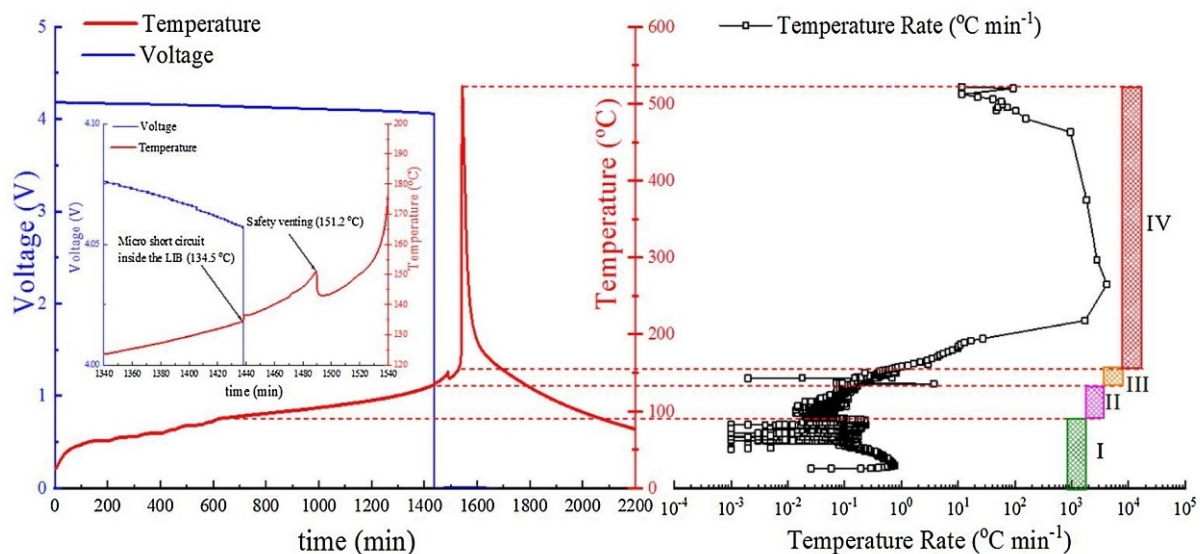


Figure 1. Voltage and temperature of temperature-induced thermal runaway [26].

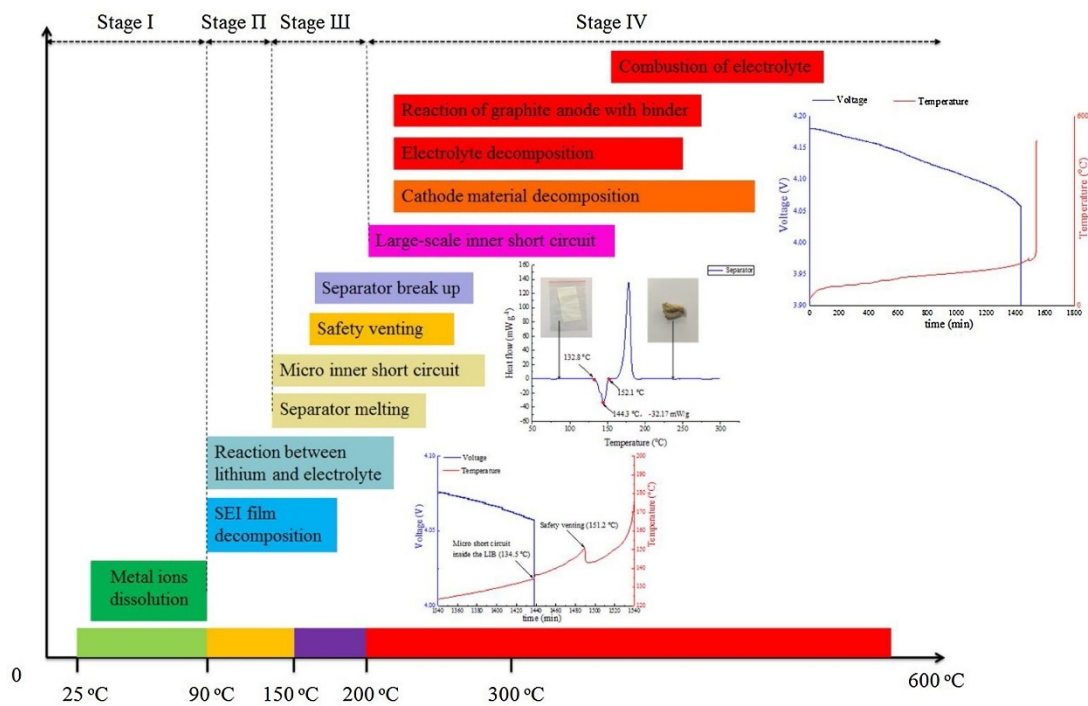


Figure 2. Stages of temperature-induced thermal runaway [26].

Li et al. [26] showed that in the room temperature (25 °C) to 90 °C region, a decrease in voltage as the temperature increases can be observed, which is caused by the dissolution of metal ions at the cathode. This is followed by the typical anode reactions of SEI decomposition and the reaction of lithium with the electrolyte above 90 °C. Of note are the spike in temperature at 134 °C, where an internal short-circuit occurs, and the small dip in temperature at 151.2 °C, where safety venting occurs. The measured value of the micro internal short-circuit is very close to the melting temperature of the separator. Cathode material decomposition is seen to occur at around 210 °C for the NMC cathode. The thermal runaway is triggered on the front surface layer and then spreads to the entire battery. The propagation time is seen to vary with SOC, as shown in Table 1 below [26].

Table 1. Effect of SOC on onset temperature of thermal runaway, propagation time in a single cell, and propagation time between cells in pack.

SOC	T Onset (°C)	Propagation Time inside a Single Cell (s)	Propagation Time between Cells (s)
100%	154.1	10	87
50%	96.3	39	307
0%	90.6	-	-

The kinetics are modeled simply as the Arrhenius equation with the basic equations presented below. Coman et al. [27] provide an overview of the basic equations used in most studies.

$$\frac{dX_a}{dt} = -A_a X_a \exp\left(-\frac{E_a}{K_b T}\right) \exp\left(-\frac{z}{z_0}\right) \quad (2)$$

$$\frac{d\alpha_c}{dt} = -A_c \alpha_c (1 - \alpha_c) \exp\left(-\frac{E_c}{K_b T}\right) \quad (3)$$

$$\frac{dX_s}{dt} = -A_s X_s \exp\left(-\frac{E_s}{K_b T}\right) \quad (4)$$

$$\frac{dz}{dt} = -A_a X_a \exp\left(-\frac{E_a}{K_b T}\right) \exp\left(-\frac{z}{z_0}\right) \quad (5)$$

Equations (2)–(4) represent the reaction rates of the anode, cathode, and SEI layer separately, while the thickness of the SEI layer is shown in Equation (5). For an unknown number of reactions with multiple unknown products, the following chemical kinetic scheme was proposed in [27]:

$$\kappa_x = A_x \cdot \exp\left(-\frac{E_{a,x}}{RT}\right) \cdot f_x(c_x) \quad (6)$$

$$c_x = 1 - \int \kappa_x dt \quad (7)$$

$$f_x(c_x) = c_x^{n_x} \quad (8)$$

where κ_x is the reaction rate, A_x is the frequency factor, $E_{a,x}$ is the activation energy, R is the universal gas constant, T is the temperature, and $f_x(c_x)$ is the mechanism function where c_x is the concentration and n_x is the reaction order. As combustion is a simple non-reversible chemical reaction, which for most abuse scenarios does not contain a mix of electrochemical and full redox reactions in parallel, the proposed kinetic scheme works well. The heat of generation is calculated as,

$$\dot{Q}_{\text{gen}} = \dot{Q}_{\text{SEI}} + \dot{Q}_{\text{An-E}} + \dot{Q}_{\text{An-B}} + \dot{Q}_{\text{Cat-An}} + \dot{Q}_{\text{Cat-B}} + \dot{Q}_{\text{Cat}} \quad (9)$$

$$\dot{Q}_x = m_x \cdot \Delta H_x \cdot \mathcal{K}_x \quad (10)$$

The thermal model is further expanded as:

$$-A\epsilon\sigma(T^4 - T_{\text{amb}}^4) - hA(T - T_{\text{amb}}) + \dot{Q}_{\text{gen}} = \rho c_p \frac{\partial T}{\partial t} \quad (11)$$

It can be seen that the model consists of an electrochemical model and a thermal model. In [27], the electrochemical model makes a significant contribution to the total heat delivered during thermal runaway. The paper modifies the electrochemical reaction term caused by the internal short-circuit device (ISCD) as it investigated thermal runaway in a pack with an ISCD. As [27] focused on internal short-circuit, the heat generated by the electrochemical reaction is included. Simply, the electrical energy of the cell is converted to heat through Joule heating, expressed as:

$$\dot{Q}_{\text{gen}} = \dot{Q}_a + \dot{Q}_c + \dot{Q}_{\text{An-B}} + \dot{Q}_s + \dot{Q}_{\text{ec}} + \dot{Q}_{\text{heater}} \quad (12)$$

$$\dot{Q}_{\text{ec}} = -H_{\text{ec}}\eta \frac{dsoc}{dt} \quad (13)$$

$$H_{\text{ec}} = 3600 \cdot C \cdot V \quad (14)$$

Jiang et al. [5] further investigated internal short-circuits with nail penetration by modifying the equation as below:

$$\dot{Q}_{\text{ec}} = -H_{\text{ec}}(1 - \eta - \gamma) \frac{dsoc}{dt} \quad (15)$$

where η is the efficiency factor for venting, and γ is the heat release factor by nail penetration. The effect of nail penetration on the outer cell casing and the thermal resistance at the

boundary was not explored. The peak temperature is estimated using the Kissinger Equation shown below:

$$\ln\left(\frac{\beta_i}{T_{p,i}^2}\right) = \ln\left(\frac{A_x R}{E_{a,x}}\right) - \frac{E_{a,x}}{RT_{p,i}}, \quad (i = 1, 2, 3, \dots) \quad (16)$$

The Biot number is a non-dimensional number that reports on the temperature uniformity and temperature gradient of the simulated element. For low Biot numbers, there is a uniform, approximately constant, temperature, while for high Biot numbers, a sharp gradient is expected. The Biot number is a major consideration in [23] where two models are proposed: the Semenov model and the Frank–Kamenetskii model. In the Semenov model, it is assumed that the distribution of temperature in the system is uniform ($Bi < 0.2$) and that heat exchange and conduction occur at the surface. The Frank–Kamenetskii model assumes that the distribution of the temperature in the system varies with space and time, with a boundary condition that the gradient of temperature is approximately zero. Typical temperature distributions from both models are shown in Figure 3 [23].

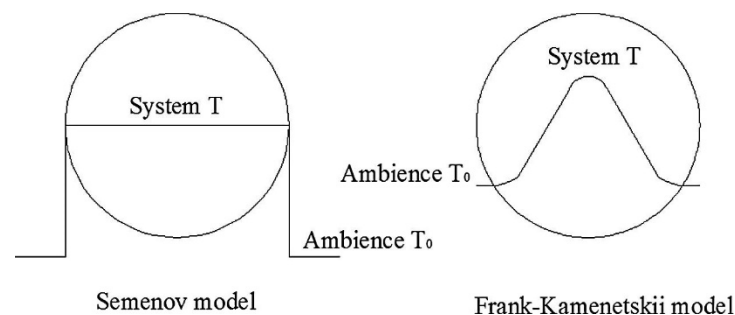


Figure 3. Temperature distributions for the Semenov and Frank–Kamenetskii models.

Huang et al. [23], using both models, calculated the self-accelerating decomposition temperature (SADT) of the cell, which is the critical temperature that triggers thermal runaway propagation, and found values of 126.1 °C and 139.2 °C for the Semenov and Frank–Kamenetskii models, respectively. The authors of the study found that when the Biot number was small ($Bi < 0.2$), the Semonov model could be used to calculate the critical temperature (SADT) of the ambient air, which was found to be 126.1 °C for the LTO electrode. While for large Biot numbers, the Frank–Kamenetskii model was used to calculate the surface temperature of the battery before self-ignition (SADT), which was found to be 142.6 °C for the LTO electrode. The study investigated the $\text{Li}_4\text{Ti}_5\text{O}_{12}$ (LTO) anode and found that the properties of LTO involving zero-strain insertion of lithium prevented lithium plating while fast charging. LTO electrodes are also noted for their thermal stability, albeit at the expense of lowered cell voltage.

The paper also reported that the SADTs for the NMC cathodes separately were 160.1 °C and 196.6 °C for the Semenov and Frank–Kamenetskii models, respectively. The authors stated that during fire engulfment the thermal resistance at the boundary can sharply decrease and that this could accelerate exothermic reactions reducing the delay time in thermal runaway. In this case (fire engulfment), the authors suggested the use of the Frank-Kamenetskii model using the Li-ion battery shell temperature as the boundary condition to calculate the SADT critical temperature. Their results showed that if the ambient temperature is more than 126.1 °C or the batteries are heated to 139.2 °C, and the time is above the delay time for thermal runaway, then thermal runaway will propagate from a cell to its surrounding cells. Moreover, if the module does not cool down to the calculated SADT's of 196.6 °C shell temperature or 160.1 °C ambient temperature, then it will be difficult to stop heat generation and venting due to NMC decomposition. However, below the critical temperature, the thermal runaway delay time is seen to approach infinity as propagation does not occur from the failing cell to the surrounding cells. The authors

also investigated two possible explanations for the causes of explosion, including internal catalytic reactions and boiling liquid expansion vapor (BLEVE).

Figure 4 shows heat flow peaks at several separate locations. A slight increase in heat generation is seen at 89.7 °C due to SEI decomposition, followed by a steady increase in heat generation as the LTO anode reacts with the electrolyte from 90 °C to 170 °C. At 171.5 °C a drop in temperature is seen as the separator melts endothermically, followed by a large spike in heat generation as the NMC cathode reacts with the electrolyte, peaking at 231.2 °C. Figure 5 breaks down this overall process further into its components. Though the heat flow term of the cathode electrolyte term is extremely large, the temperature of release is 282.8 °C, much higher than the other terms. The major contributor to the gas pressure is the electrolyte component, which is seen to experience an endothermic reaction at 187.5 °C and exothermic heat generation peak at 206.5 °C. Gachot et al. [28] state that the endothermic process is mainly the reaction of a Lewis acid with the ethylene carbonate and an elimination reaction of the Lewis acid with the solvent. The exothermic process is attributed to the decomposition of the carbonate ester. These authors also state that the amount of gas produced is directly proportional to the quantity of electrolyte. For the anode component, a small peak at 91.33 °C is attributed to the SEI decomposition. A large heat generation peak is noted at the anode that occurs after the electrolyte carbonate ester exothermic heat generation peak.

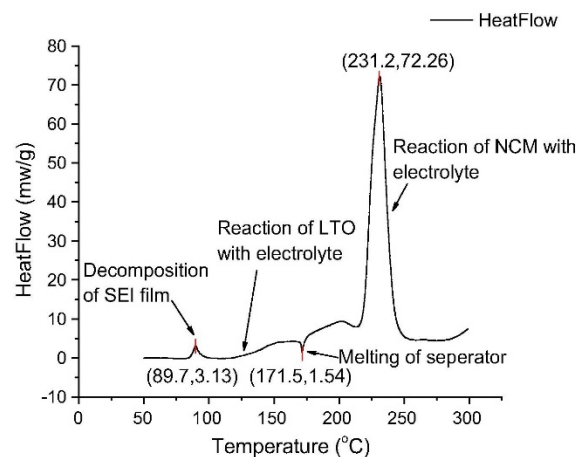


Figure 4. Heat flow vs. temperature for the entire battery [23].

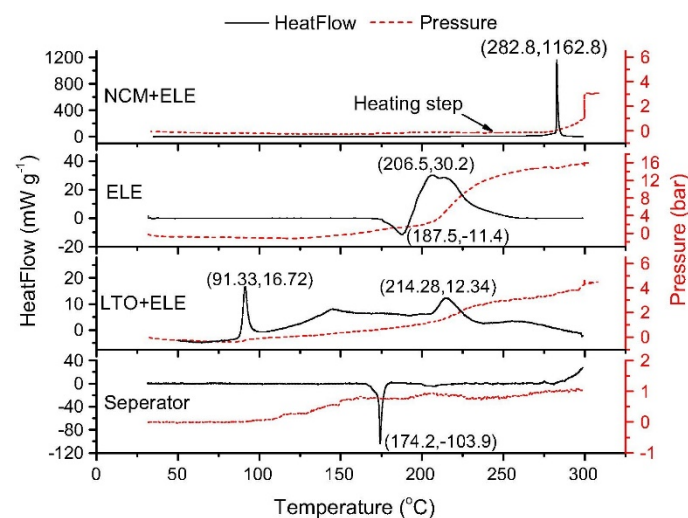


Figure 5. Heat flow vs temperature for the battery components of cathode, electrolyte, anode and separator [23].

During charging, low temperatures can lead to lithium plating, which also occurs when charging at C-rates higher than 2 C, depending on the SOC and temperature [8]. When the anode potential is negative, lithium plating can occur, as it is not the thermodynamically favored reaction. Fast charging leads to lithium plating, as interstitial sites in the graphite close to the electrolyte are occupied and prevent intercalation into deeper layers.

3.2. Other Recent Notable Studies in Thermal Runaway Modeling

Overheating is the most generic abuse condition since all battery faults lead to overheating. It is easily modeled in laboratories. Chen et al. [29] developed a lumped 0D model for small Biot number, an axisymmetric 2D model for axisymmetric heating conditions, and a 3D model for all other conditions. These models were validated by an extended volume accelerating rate calorimetry (EV-ARC) test using an NMC 2170 cylindrical cell under overheating conditions and achieved excellent agreement with experimental results. This modeling approach can be applied to different Li-ion cell chemistries and geometric configurations. Esho et al. [30] established models for two cases, including a single reaction and multiple reactions, to predict the critical temperature of thermal runaway based on a thermal balance between temperature-dependent heat generation, heat conduction in the cell, and heat dissipation on the cell surface. The model for a single reaction determines the critical temperature from the root of a nonlinear, transcendental equation whereas the model for multiple reactions is more complicated but realistic. The models were validated by the thermal test of a 2665 cylindrical cell and showed good agreement in critical temperature predictions with experimental results. The cell thermal conductivity and convective heat transfer coefficient were found to have significant influences on the critical temperature. As large format cells are gaining popularity in applications, due to their high energy per unit, a recent study conducted by Zhang et al. [13] presented a thermal runaway model for prismatic cells, validated by localized overheat testing of an LFP prismatic cell. The model was formulated based on heat generation from ISC and exothermic chemical reactions modeled by empirical Arrhenius equations. The simulated results aligned well with experimental data. Feng et al. [31] developed a comprehensive electrochemical-thermal model, which captures the thermal runaway mechanism, including capacity degradation at high temperature, ISC caused by failure of the separator, and heat generation by chemical reactions of all cell components. The model was verified with an NMC prismatic cell with close agreement obtained.

Gas generation has only rarely been considered in published thermal runaway models. Ostanek's group pioneered developing a coupled thermal and venting model and validated it using an NMC 1865 cylindrical cell under thermal abuse conditions in an EV-ARC test [32]. The model includes gas generation sources, such as vaporization of liquid electrolytes and decomposition reactions. The rate of gas generation is considered to be proportional to the rate of temperature increase. The effect after venting is also simulated in the model by producing gas, liquid, and solid ejecta from the cell, leading to losses of energy and mass from the control volume. The model agreed with experimental data for processes before and during venting up to the onset of thermal runaway, but not during the thermal runaway. The possible causes of this discrepancy might be the uncertainty of heat conduction and thermal inertia effects at rapid heating rates during thermal runaway.

Overcharge is a common electrical abuse condition. Ren et al. [33] presented an electrochemical-thermal coupled model to predict thermal runaway under overcharge conditions. The model showed close agreement with experimental data for a pair of parallel NMC pouch cells undergoing adiabatic overcharging. It was also determined by the model that electrolyte oxidation reactions, and reactions between deposited lithium and electrolyte, are the main contributors to heat generation in an overcharge process. Qi et al. [34] also formulated an overcharge model coupling a 1D electrochemical model with a 3D thermal model. It was verified by a single NMC prismatic cell, and a battery pack consisting of three NMC prismatic cells. The experimental data fitted the model well with a relative error within 6%.

External short-circuit or fast discharge-induced thermal runaway has not been studied extensively. An et al. [35] constructed an external short-circuit model for an LFP pouch and prismatic cells. The model consists of an electrochemical-thermal coupled model and an analytical thermal runaway model. The former accounts for heat generation due to ohmic heat, active polarization heat, and entropic heat, while the latter includes heat generation by decomposition reactions and predicts onset temperature and the temperature profile of thermal runaway. The electrochemical-thermal coupled model was validated using an LFP 2665 cylindrical cell under different discharge rates reported in [36]. The analytical model was verified using an 1865 cylindrical cell reported in [37]. Both results showed satisfactory agreement between simulated and experimental data.

Peng and Jiang's research established a 3D thermal model to simulate thermal runaway behaviors of cells with different cathode materials (i.e., LCO, NCA, NMC, LMO, and LFP) [38]. This research was not validated by experiments but provided a comparison between thermal stability between different cell chemistries and important parameters of the five cathode materials investigated for future studies. It was found that the heat generation rate of LFP was the slowest and, therefore, represented the safest cathode material. In [39], the authors developed a set of empirical equations to predict the thermal runaway onset temperature (TR_{onset}) of certain Li-ion batteries. The equations were third-order polynomials fitted to experimental data from external heat-induced thermal runaway on various Li-ion chemistries with multiple states of charge (SOC), where SOC was used as the independent variable. The predicted TR_{onset} had errors below 10% when compared to experimental TR_{onset} from another set of SOCs for lithium-cobalt oxide (LCO) and lithium-nickel-cobalt aluminum oxide (NCA) chemistries. Ren et al. [40] developed a model based on the reaction kinetics of the exothermic processes responsible for thermal runaway and runaway propagation. The reaction kinetics were determined via differential scanning calorimetry (DSC) and the use of Kissinger's method and a nonlinear fit. The model's ability to predict the thermal runaway onset temperature (TR_{onset}) was compared against thermal runaway data from adiabatic and oven tests. TR_{onset} was predicted with an absolute error of 9.05 °C in the adiabatic system.

ISC is the ultimate cause of thermal runaway. Coman's group modeled thermal runaway triggered by ISC and validated the model by testing an NCA 1865 cylindrical cell with a wax-based ISC device embedded in the jellyroll [41]. The model is a simplified electrochemical-thermal model constructed using Arrhenius equations for decomposition reactions and short-circuits. The experimental data matched the model well. Similarly, Cai et al. [42] developed a model to predict ISC-induced thermal runaway behavior and validated it by testing an NMC pouch cell with a wax-based ISC device embedded in the separator. This model is unique because its thermal model distinguishes the temperature among three sections of the cell, namely the core, middle, and surface layers. The overall model consists of a three-state thermal model for the three sections in the cell, a side-reaction model accounting for four exothermic decomposition reactions, and an electrical equivalent circuit model to capture the ISC process. However, the temperature data displayed relatively large differences between the simulated and experimental results mainly due to the displacement of temperature sensors during the test.

4. Lithium-Ion Battery Thermal Runaway Prognosis and Diagnosis

Thermal runaway has become a main concern for the public as the usage of Li-ion batteries has increased, especially with respect to application in EVs. Thermal runaway prognosis and diagnosis has, therefore, become an important research topic. Thermal runaway models are often used to simulate thermal runaway to validate the diagnosis approach or are sometimes used directly in the diagnosis approach. There are many recent studies on this topic; in this review, the approaches are categorized as thermal runaway prediction (prior to occurrence) and thermal runaway detection (during occurrence).

4.1. Lithium-Ion Battery Thermal Runaway Prediction

Thermal runaway prediction can be useful in terms of warning users of their abusive behaviors toward the battery or of any hostile surrounding environments around the battery. Thermal runaway can effectively be avoided by changing user behaviors or adjusting surrounding environments, which represent the best-case scenarios. If high-risk environments are unavoidable, thermal runaway mitigation approaches can be prepared to minimize damage.

Hong et al. [43] proposed a fault-detecting and fault-locating method using discrete wavelet transform (DWT) in real-time for thermal runaway prognosis. This method used a normalized discrete wavelet decomposition algorithm for real-time fault prognosis. Using data from an EV, the method successfully detected and determined the specific fault cells seven days before the thermal runaway occurred. The method was also validated against other data sets from electric vehicles. The same authors also developed a modified multiscale entropy (MMSE) algorithm to detect thermal runaway risks before the runaway occurs [44]. The method uses battery states computed in real-time via multilevel abnormality coefficients from the MMSE. The method was checked against electric vehicle data, and was also able to detect cell anomalies up to seven days before the onset of thermal runaway and could achieve the detection within the safety thresholds of the battery's state. Another study from this research group presented a new way of predicting cell voltages and detecting abnormalities using a deep learning recurrent neural network—long short-term memory (LSTM) [45]. The method uses two, many-to-one, structured LSTMs, with pre-dropout technology to prevent overfitting to data, employed separately during charging and driving. The validity and effectiveness of the method were confirmed using electric vehicle data from different seasons and driving conditions and by accurately predicting the behavior of 100 cells simultaneously.

Li et al. [46] investigated an approach to detect and locate cells with potential faults. Their method predicts cell voltages using a modified adaptive booster (MAB) based on a combination of an equivalent circuit model (ECM) and a long short-term memory (LSTM) recurrent neural network. The model's training was checked with multiple vehicle battery data and could locate a specific cell at fault 150 s before thermal runaway. The same authors proposed combined data-driven methods for a two-step thermal runaway diagnosis procedure involving temperature prediction via a modified version of extreme gradient boosting and detection of temperature irregularities using principal component analysis (PCA) and density-based spatial clustering of applications with noise (DBSCAN) [47]. The method predicted temperatures five minutes in advance with a 0.0677 mean square error. In addition, the method detected outlier cells 35 min before they underwent thermal runaway in an electric vehicle. The authors also presented a thermal runaway prognosis method which works by detecting abnormal heat generation (AHG) in the batteries [48]. The method combines a long short-term memory (LSTM) neural network with a convolutional neural network (CNN). Principal component analysis is used to lower computational time and to increase the accuracy of battery temperature prediction. AHG is measured by a model-based scheme. The prognosis method can predict temperatures up to 8 min in advance with a mean-relative-error of 0.28% and diagnosed thermal runaway 27 min before its occurrence in an electric vehicle. Another study from the same authors involved a density-based spatial clustering of applications with noise (DBSCAN) as a method for thermal runaway diagnosis [49]. Detection of individual cells at risk of runaway is performed by DBSCAN clustering used on two-dimensional fault traits. The method uses a voltage increment deviation alongside a cumulative number of deviations analysis to detect sudden and long-term deterioration, respectively. The paper affirmed that the method was able to detect individual cell deterioration a few days before thermal runaway occurred in EVs.

Klink et al. [50] compared the thermal runaway detection effectiveness of a threshold-scheme multi-sensor system with that of a model-based system in an EV battery case. The model was based on an electrical equivalent circuit model (ECM) for cell voltage and

a thermal ECM for temperature. The sensors monitored voltage, current, temperature, smoke, gas, pressure, and strain on the battery setup. Both methods detected thermal runaway more than five minutes before thermal runaway, but the model-based approach was notably faster in the tests. The same group of authors proposed a thermal fault detection method using temperature-dependent cell impedance [51]. Two equivalent circuit models (ECM) were coupled, an electrical and thermal model. Electrochemical impedance spectroscopy (EIS) was used to find the models' parameters, and its validity was checked by the worldwide harmonized light vehicles test procedure (WLTP). In the thermal abuse tests, the model was able to detect the abuse 32 min before the onset of thermal runaway.

Dong et al. [52] developed a two-stage and three-indicator method for the early detection of thermal runaway using the effects of cell deformation and cell temperature on electrochemical impedance spectroscopy (EIS). The cell temperature indicator works in an intermediate-frequency range, while the two cell deformation indicators run separately at low- and high-frequency ranges. The deformation indicators are active in the second stage which is triggered before reaching ISC temperature and thermal runaway onset temperature. Thus, the method can emit an early warning for thermal runaway. Shah et al. [53] studied a cell temperature distribution model that was designed to predict the future temperature and heat generation behavior of the cell. Their analytical model considers the effects of various decomposition reactions and the associated reactant consumption that may occur during the stages of thermal runaway. The cell's nonlinear heat generation is linearized in bounded time intervals such that temperature distribution becomes a function of time. The model's accuracy was validated via comparison with experimental measurements. The model was used to predict whether thermal runaway would occur or not in various thermal abuse tests mimicking realistic scenarios. Another study from these authors proposed a non-dimensional thermal parameter, the thermal runaway number (TRN), that could be used for thermal runaway prediction [54]. The study used an extended Semenov analysis which considers intracellular heat transfer to analyze thermal runaway. By solving the energy conservation equation governing both heat generation and removal, the TRN can be obtained. The TRN value can determine, and thus predict, whether a thermal runaway would occur.

Xiaojun et al. [55] developed a cloud-based, data-driven and model-free unsupervised clustering method for detecting thermal anomalies in Li-ion batteries. The method uses the K-shape clustering algorithm and assigns data points a membership value and distance from the center of its parent cluster. Changes in one or both of these parameters are then used to detect anomalies. The method does not require steady and significant amounts of data and outperformed vehicle BMS at detecting thermal anomalies. Jiang et al. [56] proposed a hybrid signal-based method for fault diagnosis in electric vehicle Li-ion batteries. The method uses the battery voltage signals' intrinsic mode functions which are computed by a variational mode decomposition algorithm in an outlier detection system. The outliers are categorized via density-based clustering with a Laplacian Eigen-mapping dimension reduction, and a dimensionless indicator of the voltage data. The method successfully detected a cell that culminated in thermal runaway from an electric vehicle's battery voltage time series. The authors in [57] investigated a new data-driven means for diagnosing cell-level battery pack faults and issuing thermal runaway warnings at early stages. State representation methodology (SRM) using normalized cell voltages was used to calculate and record the state of each cell in real-time. This approach successfully pinpointed specific cells and determined whether the cell fault was an over- or under-voltage fault. The method was also able to detect early thermal runaway faster than the battery management systems in the tested electric vehicles. However, in some cases, the difference in detection was only a few seconds.

4.2. Lithium-Ion Battery Internal Short-Circuit Diagnosis

The main cause of thermal runaway is ISC. Therefore, detecting ISC can also effectively prevent thermal runaway from occurring, or at least minimize its damage. Ren et al. [58] investigated the role of ISC in thermal abuse-induced thermal runaway. The 24 Ah Li-ion pouch cells were brought to a full charge with constant current constant voltage (CC-CV) charging. The cells were then heated by extended volume accelerated rate calorimetry (EV-ARC). The ISC occurred around 300 s before the runaway, and in the moments before the ISC, the resistance of the battery spiked by a factor of 1000. However, the study did not find ISC to be completely responsible for thermal runaway in a thermal abuse scenario.

Kong et al. [59] proposed a method for using time-domain data to determine impedance in a cell undergoing a micro ISC. The method used a sinusoidal output voltage variation to measure magnitude and phase response, and impedance. The method's estimated output voltages were checked against real output voltages to ensure it predicted normal cells. Thus, the proposed impedance was effectively detected by deviations in estimated and actual cell output voltage. However, the detection method was noted to have increased difficulty with large capacity cells and high-frequency voltage changes. Goa et al. [60] developed a model-based and online micro-short-circuit (MSC) analysis method to detect MSC cells in Li-ion battery packs. The authors used internal resistance and SOC difference in a cell difference model (CDM). Estimation of SOC difference was obtained using the extended Kalman filter on cell current and terminal voltage, and mean SOC data. The MSC was simulated in a 12-series-cell Li-ion pack by adding two external resistances. The model successfully detected the MSC cells and the resistance from the external resistors. Zheng et al. [61] presented an MSC detection method that uses cell SOC and cell capacity estimations to differentiate MSC from low-capacity cells in a battery pack. The method uses an extended Kalman filter with a mean difference model for estimating cell SOC incremental SOC to estimate cell capacity. Tests were conducted on four series cells with varying capacities and an external resistance connected to one of them. The method's error in capacity estimation was below 3%, and it successfully detected the MSC cell and the low-capacity cell simultaneously. Feng et al. [62] worked on an online model-based algorithm for detecting ISC. Their fault diagnosis method uses measured voltage and temperature to determine a battery's electrochemical state. The state of each battery is, hence, used in SOC difference and Ohmic heat resistance difference outlier detection methods. Based on the results of 22 substitute ISC tests, the proposed method successfully detected ISC faults before the onset of thermal runaway.

Lai et al. [63] proposed an online SOC correlated method for diagnosing ISC in its early stages. The method uses the extended Kalman filter for SOC estimations and then computes a correlation coefficient for neighboring cells with a moving window to increase accuracy. The method was compared with static leakage, SOC difference, and voltage difference methods for detecting ISC. The SOC correlation method was quicker for ISC resistances of 100 Ω and higher, and similar to the difference-based methods for lower resistances. The same authors developed a method that combines SOC difference and remaining charge capacity (RCC) while compensating for equalization electric quantity (EEQ) to detect ISC [64]. The cell mean and the cell difference models are used to compute SOC difference. The method was tested on a first-order RC model with two external resistances simulating the ISC. The RCC detection method with EEQ compensation had less than a 5% error rate; without EEQ compensation the error rate was greater than 800% for ISC with a resistance of 100+ Ω . The SOC difference detection method with EEQ compensation detected an ISC resistance of 10 Ω 6.3 h quicker than without compensation. In addition, without EEQ compensation, the SOC difference method could not detect an ISC resistance of 100 Ω or more.

Qiao et al. [65] presented a method for early diagnosis of ISCs based on their effects on incremental capacity (IC) curves. IC curves for various batteries are constructed using the extended Kalman filter. The method is based on the principle that an ISC-affected battery will require more charge to reach the same cut-off voltage as a normal cell which would

create a discrepancy in their IC curves. Tests were undertaken with external resistances and the method was able to detect batteries with ISC and to calculate the ISC resistances to quantify the magnitude of the ISC. Another study from these authors involved a mean-normalization of cloud data method for detecting ISC [66]. An adaptive Kalman filter is used on the mean-normalized voltage data to extract signs of ISC. The specific ISC cell is found via outlier detection using a density-based spatial clustering of applications with a noise (DBSCAN) algorithm. The ISC was simulated by an external resistor connected to a Li-ion cell in a 6-series cell battery pack. Using the experimental and the cloud data, the proposed method was able to detect the specific ISC cell within 2–5 h from the onset of ISC.

Schmid et al. [67] investigated a data-driven nonlinear process monitoring for the early detection of ISC in Li-ion batteries. The model is trained using an extended kernel principal component analysis (KPCA) on cell voltage difference data. A linear kernel and a radial basis function kernel are combined to obtain a wider and more sensitive range of application. The model could detect changes in a cell's rate of self-discharge and coulombic efficiency. The model was able to detect ISC in 0.7 min/Ah and 5.7 min/Ah for 10 Ω and 100 Ω resistance ISC, respectively. Ting et al. [68] worked on an ISC detection method that monitors cell voltage and cell swelling force caused by gas release. The expansion force is computed as a function of temperature and SOC, then thresholds are used to signal a fault. In tests, hard ISCs were triggered in Li-ion cells which the method detected using the expansion force and voltage monitoring in less than a second each. The authors also affirmed that the method was resistant to sensor noise. Zhenyu et al. [69] proposed a modification to their relative entropy-based early ISC detection method. The authors implemented sliding window processing with a Z-score for outlier detection to improve the accuracy and effectiveness of their relative entropy method used on cell voltage data. The method was validated with data from electric vehicles that underwent thermal runaway. The proposed method had no false positives and an accuracy rate of 98%. It performed better than the Shannon entropy method and detected short-circuit-induced runaway risks early.

4.3. Lithium-Ion Battery Thermal Runaway Detection

Thermal runaway can theoretically be prevented using the discussed thermal runaway prediction approaches as well as by ISC detection methods. However, these methods can sometimes fail to recognize the imminent threat of thermal runaway, due to unexpected factors, such as shocks and collisions, or a sudden increase in the temperature of the surroundings. Therefore, it is also important, as a last resort, to have thermal runaway detection algorithms, to warn the battery system and users of an imminent occurrence of thermal runaway, so that the damage can be minimized. Effective approaches for thermal runaway detection often involve the use of sensors.

Su et al. [70] developed a warning system based on the acoustic signal of gas venting for detecting thermal runaway in an energy storage station. The method filters out interference noise using a spectral subtraction-like denoising system. The XGBoost model is used to develop a pattern recognition classifier machine learning algorithm. The method achieved a 92.31% accuracy in detecting the thermal runaway-caused venting's acoustic signature. Li et al. [71] compared the effectiveness of internal resistance temperature detectors (RTD) and surface temperature sensors at detecting overcharge-induced thermal runaway in Li-ion pouch cells. The cells were overcharged at 1 C and 5 C rates until the cell exploded. It was found that the internal RTDs detected the solid-electrolyte interface (SEI) degradation onset temperature around 10 s quicker than the surface sensors. The internal temperature monitoring was also more reliable than the surface monitoring. Sheikh et al. [72] used a numerical simulation to detect thermal runaway in an analysis of mechanical failure caused by four kinds of quasi-static loading conditions. The simulated cell was modeled by finite element analysis. The results were checked against voltage and temperature measurements from the experimental data. The numerical simulations of temperature and applied force

behavior were within 10% of the experimental findings. The various loading conditions were found to be effective for detecting the signs of runaway.

Koch et al. [73] determined the effectiveness and viability of seven kinds of sensors for detecting thermal runaway in Li-ion traction batteries caused by overheating or mechanical penetration. The sensors were as follows: voltage sensor, gas sensor, smoke detector, creep distance sensor, temperature sensor, absolute pressure sensor, and piezoresistive force sensor. The measured criteria were detection speed, signal clarity, and characteristics such as sensor implementation, size, and power consumption. All sensors succeeded in detecting thermal runaway with no restriction with respect to battery size or energy density. No individual sensor satisfied all criteria; instead, the use of multiple sensors, which compensated for underperforming elements, was suggested. Cai et al. [74] compared the ability of a gas sensor with that of a surface temperature sensor to detect cell-short-circuit-induced thermal runaway before the runaway propagates to neighboring cells in a sizeable battery storage vessel. Surface temperature measurement was incapable of detecting thermal runaway before propagation. In contrast, the gas sensor which measured the CO₂ gas concentration was able to determine the presence of cell thermal runaway in 85 s. This detection speed was significantly shorter than the time needed for runaway propagation which was evaluated at 710 s. He et al. [75] proposed a hierarchical warning system based on sensor readings to detect and signal the onset of thermal runaway before it is irreversible. Temperature, gas, smoke and infrared sensors were the various types of alert sensors used. The system sets thresholds that need to be crossed before moving up a four-tiered communication and response hierarchy. The number of sensors and their placement were designed to increase safety and efficiency. As such, the system was able to rapidly determine where the initial stages of thermal runaway were beginning to occur.

5. Conclusions

The safety of Li-ion batteries has become an important field of research due to their increasing usage in various practical applications. Thermal runaway is among the biggest safety concerns involving Li-ion batteries, since it can lead to fires or explosions. Thermal runaway modeling, as well as thermal runaway prediction and detection, are important research topics that can help prevent or mitigate the consequences of thermal runaway. This paper provides a comprehensive review of existing thermal runaway modeling approaches, and prognostic and diagnostic methods for Li-ion battery systems. The summary of models, algorithms and approaches provided in this review serves as a basis for researchers to develop more effective modeling and diagnostic methods for Li-ion battery thermal runaway in the future to improve battery safety.

Author Contributions: Conceptualization, M.-K.T. and M.F.; methodology, S.P., Y.X. and M.F.; formal analysis, M.-K.T. and A.M.; writing—original draft preparation, M.-K.T., A.A. and A.M.; writing—review and editing, S.P., Y.X. and M.F.; visualization, A.M.; supervision, M.F. All authors have read and agreed to the published version of the manuscript.

Funding: This research received no external funding.

Conflicts of Interest: The authors declare no conflict of interest.

References

1. Tran, M.-K.; Sherman, S.; Samadani, E.; Vrolyk, R.; Wong, D.; Lowery, M.; Fowler, M. Environmental and Economic Benefits of a Battery Electric Vehicle Powertrain with a Zinc–Air Range Extender in the Transition to Electric Vehicles. *Vehicles* **2020**, *2*, 398–412. [[CrossRef](#)]
2. Tran, M.-K.; DaCosta, A.; Mevawalla, A.; Panchal, S.; Fowler, M. Comparative Study of Equivalent Circuit Models Performance in Four Common Lithium-Ion Batteries: LFP, NMC, LMO, NCA. *Batteries* **2021**, *7*, 51. [[CrossRef](#)]
3. Tran, M.-K.; Akinsanya, M.; Panchal, S.; Fraser, R.; Fowler, M. Design of a Hybrid Electric Vehicle Powertrain for Performance Optimization Considering Various Powertrain Components and Configurations. *Vehicles* **2021**, *3*, 20–32. [[CrossRef](#)]
4. Tran, M.-K.; Cunanan, C.; Panchal, S.; Fraser, R.; Fowler, M. Investigation of Individual Cells Replacement Concept in Lithium-Ion Battery Packs with Analysis on Economic Feasibility and Pack Design Requirements. *Processes* **2021**, *9*, 2263. [[CrossRef](#)]

5. Jiang, Z.Y.; Qu, Z.G.; Zhang, J.F.; Rao, Z.H. Rapid Prediction Method for Thermal Runaway Propagation in Battery Pack Based on Lumped Thermal Resistance Network and Electric Circuit Analogy. *Appl. Energy* **2020**, *268*, 115007. [[CrossRef](#)]
6. Tran, M.-K.; Mathew, M.; Janhunen, S.; Panchal, S.; Raahemifar, K.; Fraser, R.; Fowler, M. A comprehensive equivalent circuit model for lithium-ion batteries, incorporating the effects of state of health, state of charge, and temperature on model parameters. *J. Energy Storage* **2021**, *43*, 103252. [[CrossRef](#)]
7. IEA. Global EV Outlook. 2021. Available online: <https://www.iea.org/reports/global-ev-outlook-2021> (accessed on 8 February 2022).
8. Tran, M.-K.; Fowler, M. A Review of Lithium-Ion Battery Fault Diagnostic Algorithms: Current Progress and Future Challenges. *Algorithms* **2020**, *13*, 62. [[CrossRef](#)]
9. Tran, M.-K.; Panchal, S.; Khang, T.D.; Panchal, K.; Fraser, R.; Fowler, M. Concept Review of a Cloud-Based Smart Battery Management System for Lithium-Ion Batteries: Feasibility, Logistics, and Functionality. *Batteries* **2022**, *8*, 19. [[CrossRef](#)]
10. Tran, M.-K.; Fowler, M. Sensor Fault Detection and Isolation for Degrading Lithium-Ion Batteries in Electric Vehicles Using Parameter Estimation with Recursive Least Squares. *Batteries* **2020**, *6*, 1. [[CrossRef](#)]
11. Xie, Y.; Li, H.; Li, W.; Zhang, Y.; Fowler, M.; Tran, M.-K.; Zhang, X.; Chen, B.; Deng, S. Improving thermal performance of battery at high current rate by using embedded heat pipe system. *J. Energy Storage* **2022**, *46*, 103809. [[CrossRef](#)]
12. Feng, X.; Ouyang, M.; Liu, X.; Lu, L.; Xia, Y.; He, X. Thermal Runaway Mechanism of Lithium Ion Battery for Electric Vehicles: A Review. *Energy Storage Mater.* **2018**, *10*, 246–267. [[CrossRef](#)]
13. Tran, M.-K.; Panchal, S.; Chauhan, V.; Brahmabhatt, N.; Mevawalla, A.; Fraser, R.; Fowler, M. Python-based scikit-learn machine learning models for thermal and electrical performance prediction of high-capacity lithium-ion battery. *Int. J. Energy Res.* **2021**, *12*, 2825. [[CrossRef](#)]
14. Xiong, R.; Ma, S.; Li, H.; Sun, F.; Li, J. Toward a Safer Battery Management System: A Critical Review on Diagnosis and Prognosis of Battery Short Circuit. *iScience* **2020**, *23*, 101010. [[CrossRef](#)] [[PubMed](#)]
15. Zhang, G.; Wei, X.; Tang, X.; Zhu, J.; Chen, S.; Dai, H. Internal Short Circuit Mechanisms, Experimental Approaches and Detection Methods of Lithium-Ion Batteries for Electric Vehicles: A Review. *Renew. Sustain. Energy Rev.* **2021**, *141*, 110790. [[CrossRef](#)]
16. Huang, L.; Liu, L.; Lu, L.; Feng, X.; Han, X.; Li, W.; Zhang, M.; Li, D.; Liu, X.; Sauer, D.U.; et al. A Review of the Internal Short Circuit Mechanism in Lithium-Ion Batteries: Inducement, Detection and Prevention. *Int. J. Energy Res.* **2021**, *45*, 15797–15831. [[CrossRef](#)]
17. Liao, Z.; Zhang, S.; Li, K.; Zhang, G.; Habetler, T.G. A Survey of Methods for Monitoring and Detecting Thermal Runaway of Lithium-Ion Batteries. *J. Power Sources* **2019**, *2019*, 436. [[CrossRef](#)]
18. Feng, X.; Zheng, S.; Ren, D.; He, X.; Wang, L.; Liu, X.; Li, M.; Ouyang, M. Key Characteristics for Thermal Runaway of Li-Ion Batteries. *Energy Procedia* **2019**, *158*, 4684–4689. [[CrossRef](#)]
19. Yuan, C.; Wang, Q.; Wang, Y.; Zhao, Y. Inhibition Effect of Different Interstitial Materials on Thermal Runaway Propagation in the Cylindrical Lithium-Ion Battery Module. *Appl. Therm. Eng.* **2019**, *153*, 39–50. [[CrossRef](#)]
20. Wang, Q.; Jiang, B.; Li, B.; Yan, Y. A Critical Review of Thermal Management Models and Solutions of Lithium-Ion Batteries for the Development of Pure Electric Vehicles. *Renew. Sustain. Energy Rev.* **2016**, *64*, 106–128. [[CrossRef](#)]
21. Bandhauer, T.M.; Garimella, S.; Fuller, T.F. A Critical Review of Thermal Issues in Lithium-Ion Batteries. *J. Electrochem. Soc.* **2011**, *158*, R1. [[CrossRef](#)]
22. Ma, S.; Jiang, M.; Tao, P.; Song, C.; Wu, J.; Wang, J.; Deng, T.; Shang, W. Temperature Effect and Thermal Impact in Lithium-Ion Batteries: A Review. *Prog. Nat. Sci. Mater. Int.* **2018**, *28*, 653–666. [[CrossRef](#)]
23. Huang, P.; Ping, P.; Li, K.; Chen, H.; Wang, Q.; Wen, J.; Sun, J. Experimental and Modeling Analysis of Thermal Runaway Propagation over the Large Format Energy Storage Battery Module with $\text{Li}_4\text{Ti}_5\text{O}_{12}$ Anode. *Appl. Energy* **2016**, *183*, 659–673. [[CrossRef](#)]
24. Liu, X.; Stolarov, S.I.; Denlinger, M.; Masias, A.; Snyder, K. Comprehensive Calorimetry of the Thermally-Induced Failure of a Lithium Ion Battery. *J. Power Sources* **2015**, *280*, 516–525. [[CrossRef](#)]
25. Feng, X.; Sun, J.; Ouyang, M.; He, X.; Lu, L.; Han, X.; Fang, M.; Peng, H. Characterization of Large Format Lithium Ion Battery Exposed to Extremely High Temperature. *J. Power Sources* **2014**, *272*, 457–467. [[CrossRef](#)]
26. Li, H.; Duan, Q.; Zhao, C.; Huang, Z.; Wang, Q. Experimental Investigation on the Thermal Runaway and Its Propagation in the Large Format Battery Module with $\text{Li}(\text{Ni}_{1/3}\text{Co}_{1/3}\text{Mn}_{1/3})\text{O}_2$ as Cathode. *J. Hazard. Mater.* **2019**, *375*, 241–254. [[CrossRef](#)] [[PubMed](#)]
27. Coman, P.T.; Darcy, E.C.; Veje, C.T.; White, R.E. Numerical Analysis of Heat Propagation in a Battery Pack Using a Novel Technology for Triggering Thermal Runaway. *Appl. Energy* **2017**, *203*, 189–200. [[CrossRef](#)]
28. Gachot, G.; Grugeon, S.; Armand, M.; Pilard, S.; Guenot, P.; Tarascon, J.M.; Laruelle, S. Deciphering the Multi-Step Degradation Mechanisms of Carbonate-Based Electrolyte in Li Batteries. *J. Power Sources* **2008**, *178*, 409–421. [[CrossRef](#)]
29. Chen, H.; Buston, J.E.H.; Gill, J.; Howard, D.; Williams, R.C.E.; Read, E.; Abaza, A.; Cooper, B.; Wen, J.X. A Simplified Mathematical Model for Heating-Induced Thermal Runaway of Lithium-Ion Batteries. *J. Electrochem. Soc.* **2021**, *168*, 010502. [[CrossRef](#)]
30. Esho, I.; Shah, K.; Jain, A. Measurements and Modeling to Determine the Critical Temperature for Preventing Thermal Runaway in Li-Ion Cells. *Appl. Therm. Eng.* **2018**, *145*, 287–294. [[CrossRef](#)]
31. Feng, X.; He, X.; Ouyang, M.; Wang, L.; Lu, L.; Ren, D.; Santhanagopalan, S. A Coupled Electrochemical-Thermal Failure Model for Predicting the Thermal Runaway Behavior of Lithium-Ion Batteries. *J. Electrochem. Soc.* **2018**, *165*, A3748–A3765. [[CrossRef](#)]

32. Ostanek, J.K.; Li, W.; Mukherjee, P.P.; Crompton, K.R.; Hacker, C. Simulating Onset and Evolution of Thermal Runaway in Li-Ion Cells Using a Coupled Thermal and Venting Model. *Appl. Energy* **2020**, *268*, 114972. [[CrossRef](#)]
33. Ren, D.; Feng, X.; Lu, L.; Ouyang, M.; Zheng, S.; Li, J.; He, X. An Electrochemical-Thermal Coupled Overcharge-to-Thermal-Runaway Model for Lithium Ion Battery. *J. Power Sources* **2017**, *364*, 328–340. [[CrossRef](#)]
34. Qi, C.; Zhu, Y.; Gao, F.; Yang, K.; Jiao, Q. Mathematical Model for Thermal Behavior of Lithium Ion Battery Pack under Overcharge. *Int. J. Heat Mass Transf.* **2018**, *124*, 552–563. [[CrossRef](#)]
35. An, Z.; Shah, K.; Jia, L.; Ma, Y. Modeling and Analysis of Thermal Runaway in Li-Ion Cell. *Appl. Therm. Eng.* **2019**, *160*, 113960. [[CrossRef](#)]
36. Drake, S.J.; Martin, M.; Wetz, D.A.; Ostanek, J.K.; Miller, S.P.; Heinzl, J.M.; Jain, A. Heat Generation Rate Measurement in a Li-Ion Cell at Large C-Rates through Temperature and Heat Flux Measurements. *J. Power Sources* **2015**, *285*, 266–273. [[CrossRef](#)]
37. Hatchard, T.D.; MacNeil, D.D.; Basu, A.; Dahn, J.R. Thermal Model of Cylindrical and Prismatic Lithium-Ion Cells. *J. Electrochem. Soc.* **2001**, *148*, A755–A761. [[CrossRef](#)]
38. Peng, P.; Jiang, F. Thermal Safety of Lithium-Ion Batteries with Various Cathode Materials: A Numerical Study. *Int. J. Heat Mass Transf.* **2016**, *103*, 1008–1016. [[CrossRef](#)]
39. Chombo, P.V.; Laonual, Y. Prediction of the Onset of Thermal Runaway and Its Thermal Hazards in 18650 Lithium-Ion Battery Abused by External Heating. *Fire Saf. J.* **2022**, *129*, 103560. [[CrossRef](#)]
40. Ren, D.; Liu, X.; Feng, X.; Lu, L.; Ouyang, M.; Li, J.; He, X. Model-Based Thermal Runaway Prediction of Lithium-Ion Batteries from Kinetics Analysis of Cell Components. *Appl. Energy* **2018**, *228*, 633–644. [[CrossRef](#)]
41. Coman, P.T.; Darcy, E.C.; Veje, C.T.; White, R.E. Modelling Li-Ion Cell Thermal Runaway Triggered by an Internal Short Circuit Device Using an Efficiency Factor and Arrhenius Formulations. *J. Electrochem. Soc.* **2017**, *164*, A587–A593. [[CrossRef](#)]
42. Cai, T.; Stefanopoulou, A.G.; Siegel, J.B. Modeling Li-Ion Battery Thermal Runaway Using a Three Section Thermal Model. In Proceedings of the ASME 2018 Dynamic Systems and Control Conference, DSCC 2018, Atlanta, GA, USA, 30 September–3 October 2018; Volume 2.
43. Hong, J.; Wang, Z.; Qu, C.; Ma, F.; Xu, X.; Yang, J.; Zhang, J.; Zhou, Y.; Shan, T.; Hou, Y. Fault Prognosis and Isolation of Lithium-Ion Batteries in Electric Vehicles Considering Real-Scenario Thermal Runaway Risks. *IEEE J. Emerg. Sel. Top. Power Electron.* **2021**, *1*. [[CrossRef](#)]
44. Hong, J.; Wang, Z.; Ma, F.; Yang, J.; Xu, X.; Qu, C.; Zhang, J.; Shan, T.; Hou, Y.; Zhou, Y. Thermal Runaway Prognosis of Battery Systems Using the Modified Multiscale Entropy in Real-World Electric Vehicles. *IEEE Trans. Transp. Electrifi.* **2021**, *7*, 2269–2278. [[CrossRef](#)]
45. Hong, J.; Wang, Z.; Yao, Y. Fault Prognosis of Battery System Based on Accurate Voltage Abnormality Prognosis Using Long Short-Term Memory Neural Networks. *Appl. Energy* **2019**, *251*, 113381. [[CrossRef](#)]
46. Li, D.; Zhang, Z.; Liu, P.; Wang, Z.; Zhang, L. Battery Fault Diagnosis for Electric Vehicles Based on Voltage Abnormality by Combining the Long Short-Term Memory Neural Network and the Equivalent Circuit Model. *IEEE Trans. Power Electron.* **2021**, *36*, 1303–1315. [[CrossRef](#)]
47. Li, D.; Zhang, Z.; Wang, Z.; Liu, P.; Liu, Z.; Lin, N. Timely Thermal Runaway Prognosis for Battery Systems in Real-World Electric Vehicles Based on Temperature Abnormality. *IEEE J. Emerg. Sel. Top. Power Electron.* **2022**, *1*. [[CrossRef](#)]
48. Li, D.; Liu, P.; Zhang, Z.; Zhang, L.; Deng, J.; Wang, Z.; Dorrell, D.G.; Li, W.; Sauer, D.U. Battery Thermal Runaway Fault Prognosis in Electric Vehicles Based on Abnormal Heat Generation and Deep Learning Algorithms. *IEEE Trans. Power Electron.* **2022**, *37*, 8513–8525. [[CrossRef](#)]
49. Li, D.; Zhang, Z.; Liu, P.; Wang, Z. DBSCAN-Based Thermal Runaway Diagnosis of Battery Systems for Electric Vehicles. *Energies* **2019**, *12*, 2977. [[CrossRef](#)]
50. Klink, J.; Hebenbrock, A.; Grabow, J.; Orazov, N.; Nylén, U.; Bengler, R.; Beck, H.-P. Comparison of Model-Based and Sensor-Based Detection of Thermal Runaway in Li-Ion Battery Modules for Automotive Application. *Batteries* **2022**, *8*, 34. [[CrossRef](#)]
51. Klink, J.; Grabow, J.; Orazov, N.; Bengler, R.; Börger, A.; Ahlberg Tidblad, A.; Wenzl, H.; Beck, H.P. Thermal Fault Detection by Changes in Electrical Behaviour in Lithium-Ion Cells. *J. Power Sources* **2021**, *490*, 229572. [[CrossRef](#)]
52. Dong, P.; Liu, Z.; Wu, P.; Li, Z.; Wang, Z.; Zhang, J. Reliable and Early Warning of Lithium-Ion Battery Thermal Runaway Based on Electrochemical Impedance Spectrum. *J. Electrochem. Soc.* **2021**, *168*, 090529. [[CrossRef](#)]
53. Shah, K.; Jain, A. Prediction of Thermal Runaway and Thermal Management Requirements in Cylindrical Li-Ion Cells in Realistic Scenarios. *Int. J. Energy Res.* **2019**, *43*, 1827–1838. [[CrossRef](#)]
54. Shah, K.; Chalise, D.; Jain, A. Experimental and Theoretical Analysis of a Method to Predict Thermal Runaway in Li-Ion Cells. *J. Power Sources* **2016**, *330*, 167–174. [[CrossRef](#)]
55. Li, X.; Li, J.; Abdollahi, A.; Jones, T. Data-Driven Thermal Anomaly Detection for Batteries Using Unsupervised Shape Clustering. In Proceedings of the IEEE International Symposium on Industrial Electronics, Kyoto, Japan, 20–23 June 2021.
56. Jiang, J.; Cong, X.; Li, S.; Zhang, C.; Zhang, W.; Jiang, Y. A Hybrid Signal-Based Fault Diagnosis Method for Lithium-Ion Batteries in Electric Vehicles. *IEEE Access* **2021**, *9*, 19175–19186. [[CrossRef](#)]
57. Jiang, L.; Deng, Z.; Tang, X.; Hu, L.; Lin, X.; Hu, X. Data-Driven Fault Diagnosis and Thermal Runaway Warning for Battery Packs Using Real-World Vehicle Data. *Energy* **2021**, *234*, 121266. [[CrossRef](#)]

58. Ren, D.; Feng, X.; Liu, L.; Hsu, H.; Lu, L.; Wang, L.; He, X.; Ouyang, M. Investigating the Relationship between Internal Short Circuit and Thermal Runaway of Lithium-Ion Batteries under Thermal Abuse Condition. *Energy Storage Mater.* **2021**, *34*, 563–573. [[CrossRef](#)]
59. Kong, X.; Plett, G.L.; Scott Trimboli, M.; Zhang, Z.; Qiao, D.; Zhao, T.; Zheng, Y. Pseudo-Two-Dimensional Model and Impedance Diagnosis of Micro Internal Short Circuit in Lithium-Ion Cells. *J. Energy Storage* **2020**, *27*, 101085. [[CrossRef](#)]
60. Gao, W.; Zheng, Y.; Ouyang, M.; Li, J.; Lai, X.; Hu, X. Micro-Short-Circuit Diagnosis for Series-Connected Lithium-Ion Battery Packs Using Mean-Difference Model. *IEEE Trans. Ind. Electron.* **2019**, *66*, 2132–2214. [[CrossRef](#)]
61. Zheng, Y.; Luo, Q.; Cui, Y.; Dai, H.; Han, X.; Feng, X. Fault Identification and Quantitative Diagnosis Method for Series-Connected Lithium-Ion Battery Packs Based on Capacity Estimation. *IEEE Trans. Ind. Electron.* **2022**, *69*, 3059–3067. [[CrossRef](#)]
62. Feng, X.; Pan, Y.; He, X.; Wang, L.; Ouyang, M. Detecting the Internal Short Circuit in Large-Format Lithium-Ion Battery Using Model-Based Fault-Diagnosis Algorithm. *J. Energy Storage* **2018**, *18*, 26–39. [[CrossRef](#)]
63. Lai, X.; Yi, W.; Kong, X.; Han, X.; Zhou, L.; Sun, T.; Zheng, Y. Online Detection of Early Stage Internal Short Circuits in Series-Connected Lithium-Ion Battery Packs Based on State-of-Charge Correlation. *J. Energy Storage* **2020**, *30*, 101514. [[CrossRef](#)]
64. Lai, X.; Yi, W.; Li, H.; Han, X.; Feng, X.; Li, S.; Zhou, L.; Zheng, Y. Online Internal Short Circuit Detection Method Considering Equalization Electric Quantity for Lithium-Ion Battery Pack in Electric Vehicles. *Int. J. Energy Res.* **2021**, *45*, 7326–7340. [[CrossRef](#)]
65. Qiao, D.; Wang, X.; Lai, X.; Zheng, Y.; Wei, X.; Dai, H. Online Quantitative Diagnosis of Internal Short Circuit for Lithium-Ion Batteries Using Incremental Capacity Method. *Energy* **2022**, *243*, 123082. [[CrossRef](#)]
66. Qiao, D.; Wei, X.; Fan, W.; Jiang, B.; Lai, X.; Zheng, Y.; Tang, X.; Dai, H. Toward Safe Carbon-Neutral Transportation: Battery Internal Short Circuit Diagnosis Based on Cloud Data for Electric Vehicles. *Appl. Energy* **2022**, *317*, 119168. [[CrossRef](#)]
67. Schmid, M.; Kleiner, J.; Endisch, C. Early Detection of Internal Short Circuits in Series-Connected Battery Packs Based on Nonlinear Process Monitoring. *J. Energy Storage* **2022**, *48*, 103732. [[CrossRef](#)]
68. Cai, T.; Pannala, S.; Stefanopoulou, A.G.; Siegel, J.B. Battery Internal Short Detection Methodology Using Cell Swelling Measurements. In Proceedings of the American Control Conference, Denver, CO, USA, 1–3 July 2020.
69. Sun, Z.; Wang, Z.; Chen, Y.; Liu, P.; Wang, S.; Zhang, Z.; Dorrell, D.G. Modified Relative Entropy Based Lithium-Ion Battery Pack Online Short Circuit Detection for Electric Vehicle. *IEEE Trans. Transp. Electrif.* **2021**, *8*, 1710–1723. [[CrossRef](#)]
70. Su, T.; Lyu, N.; Zhao, Z.; Wang, H.; Jin, Y. Safety Warning of Lithium-Ion Battery Energy Storage Station via Venting Acoustic Signal Detection for Grid Application. *J. Energy Storage* **2021**, *38*, 102498. [[CrossRef](#)]
71. Li, B.; Parekh, M.H.; Pol, V.G.; Adams, T.E.; Fleetwood, J.; Jones, C.M.; Tomar, V. Operando Monitoring of Electrode Temperatures During Overcharge-Caused Thermal Runaway. *Energy Technol.* **2021**, *9*, 2100497. [[CrossRef](#)]
72. Sheikh, M.; Elmarakbi, A.; Elkady, M. Thermal Runaway Detection of Cylindrical 18650 Lithium-Ion Battery under Quasi-Static Loading Conditions. *J. Power Sources* **2017**, *370*, 61–70. [[CrossRef](#)]
73. Koch, S.; Birke, K.P.; Kuhn, R. Fast Thermal Runaway Detection for Lithium-Ion Cells in Large Scale Traction Batteries. *Batteries* **2018**, *4*, 16. [[CrossRef](#)]
74. Cai, T.; Stefanopoulou, A.G.; Siegel, J.B. Early Detection for Li-Ion Batteries Thermal Runaway Based on Gas Sensing. *ECS Trans.* **2019**, *89*, 85–97. [[CrossRef](#)]
75. He, D.; Sun, J.; Li, Y.; Tian, F.; Chen, Y.; Tong, G.; Chen, X.; Shen, Q.; Lian, Z. Thermal Runaway Warning Based on Safety Management System of Lithium Iron Phosphate Battery for Energy Storage. In Proceedings of the 2020 IEEE International Conference on Artificial Intelligence and Information Systems, ICAIIS 2020, Dalian, China, 20–22 March 2020.